

Electrical detection of single-base DNA mutation using functionalized nanoparticles

Mohammud R. Noor,^{1,2} Swati Goyal,^{2,3} Shawn M. Christensen,⁴ and Samir M. Iqbal^{1,2,5,a)}

¹Department of Electrical Engineering, The University of Texas at Arlington, Arlington, Texas 76019, USA

²Nanotechnology Research and Teaching Facility, The University of Texas at Arlington, Arlington, Texas 76019, USA

³Department of Bioengineering, The University of Texas at Arlington, Arlington, Texas 76019, USA

⁴Department of Biology, The University of Texas at Arlington, Arlington, Texas 76019, USA

⁵Joint Graduate Committee of Biomedical Engineering Program, University of Texas at Arlington and University of Texas Southwestern Medical Center at Dallas, Arlington, Texas 76019 USA

(Received 25 March 2009; accepted 18 May 2009; published online 17 August 2009)

We report an electrical scheme to detect specific DNA. Engineered hairpin probe DNA are immobilized on a silicon chip between gold nanoelectrodes. Hybridization of target DNA to the hairpin melts the stem nucleotides. Gold nanoparticle-conjugated universal reporter sequence detects the open hairpins by annealing to the exposed stem nucleotides. The gold nanoparticles increase charge conduction between the electrodes. Specifically, we report on a hairpin probe designed to detect a medically relevant mutant form of the *K-ras* oncogene. Direct current measurements show three orders of magnitude increase in conductivity for as low as 2 fmol of target molecules. © 2009 American Institute of Physics. [DOI: 10.1063/1.3152768]

Individual genetic mutations can predispose a cell or tissue toward cancer. High throughput screening has identified altered genes in many spontaneous as well as hereditary cancers.^{1,2} For example, mutations in base 12 of the *K-ras* gene are implicated in over 90% of pancreatic carcinomas, and it is also considered a prognostic indicator for lung cancer patients.³ Specific mutations in such genes can thus be used as diagnostic indicators for the susceptibility of disease, aiding in early detection and treatment.⁴

Microarrays are a common method to screen for the presence or absence of particular genomic sequences. Microarrays use single stranded DNA probes attached to chips to capture fluorescently tagged genomic DNA. The fluorescent markers are excited for detection. Fluorescent tags, however, can affect the stability and fidelity of the probe-target interactions, thereby reducing reliability.⁵ To overcome this (and other) inherent limitation(s), we report an alternative probe and detection method—hairpin DNA probe instead of single stranded linear DNA, and electrical detection instead of fluorescent detection, with single-base mismatch sensitivity down to 2 fmol of target DNA. Previous experiments along these lines have demonstrated the potential of hairpin probes to improve reliability and fidelity of microarrays. In addition, a number of alternative detection mechanisms have been reported with the detection limits between a few nmol and 1.8 fmol:^{6–8} impedance measurements,⁹ capacitance detection,¹⁰ cyclic voltammeter measurements,¹¹ and calorimetric measurements.

We attach a hairpin probe to a silicon oxide surface located between two isolated nanoelectrodes (Fig. 1). The loop of the hairpin and one stem forming segment is complementary to the DNA of interest. The other side of the hairpin stem is complementary to an engineered reporter oligonucleotide (called GNP-reporter). The GNP-reporter is conjugated

to a gold-nanoparticle (GNP). When the DNA of interest hybridizes to the loop, the stem of the hairpin probe destabilizes and melts. Electrical detection of the hairpin opening is conferred upon the system by the ability of the GNP-reporter to conduct electricity between the nanoelectrodes upon annealing to the exposed stem.

The DNA oligonucleotides used in this study (Table I) were purchased from Sigma Aldrich (Saint Louis, MO). The oligonucleotides are given the names “hairpin probe,” “PC-target,” “MM-target,” and “GNP-reporter” based on their roles. Hairpin probe consists of a three nucleotide spacer, a 12 nucleotide loop, and a six base pair (bp) stem. The target DNA, PC-target and MM-target, are identical to

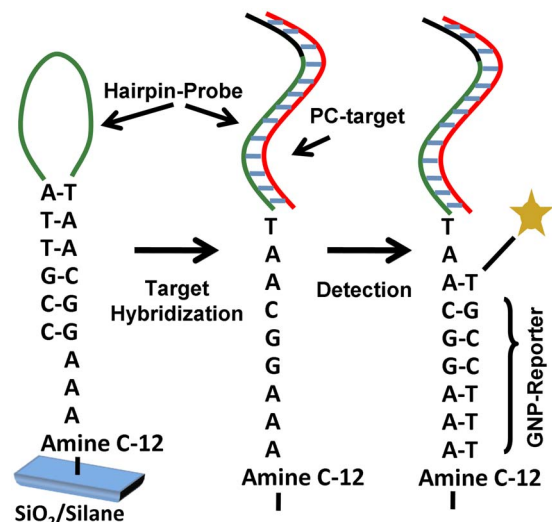


FIG. 1. (Color online) Schematics showing reporter sequence carrying the gold nanoparticle (yellow star) binding to the hairpin probe after complementary DNA (PC-target, red) interacts with the loop (green) of the hairpin. The PC-target starts with GGCAA and covers the whole loop. Black portion depicts the part of hairpin that formed the stem before opening.

^{a)}Electronic mail: smiqbal@uta.edu.

TABLE I. DNA sequences and their modifications.

Sequence Name	Oligonucleotide (5' to 3')	Modification
Hairpin Probe	AAAGGCAATTTCCGCCGCCATTGCC	5' C12 Amine
PC-target	GGC AAT GGC GGC GGC GAA	None
MM-target	GGC AGT GGC GGC GGC GAA	None
GNP-reporter	TGCCTTT	5' Thiol and GNP

each other except at one position (marked in bold in Table I). PC-target, the mutated version of the oncogene, is perfect-complementary to the hairpin probe loop and one stem forming side. MM-target is the 18 bp wild type DNA taken from *K-ras* oncogene. The MM-target is unable to open and hybridize the hairpin probe while PC-target (the mutant) opens the hairpin structure and forms a duplex (Fig. 1). The seven base GNP-reporter increases the detection limit of the system by increasing electrical conductance across the nanoelectrodes when the hairpin is in the open configuration. Our approach can be used, in principle, to electrically detect any specific oncogene or mutation.

Thermodynamically, the probe DNA forms a strong hairpin loop structure with stem size of six bp having ΔG_{probe} of -4.42 kcal/mol at 25°C .¹² PC-target binds to the probe molecule with ΔG_{PC} of -24.45 kcal/mol. MM-target has calculated ΔG_{MM} of -21.20 kcal/mol. The reduced ΔG for MM fails to overcome the hairpin conformation, indicating hairpin structure has a lot more free energy penalty to overcome for a MM than what is calculated by standard formulas. The equilibrium equations associated with PC and MM interactions with a hairpin probe in closed loop form (PR) can be written as $\text{PC} + \text{PR} \rightarrow \text{PC}_{\text{duplex}}$ and $\text{MM} + \text{PR} \rightarrow \text{MM}_{\text{duplex}}$ (with respective reaction free energies ΔG_{PC} and ΔG_{MM}).¹⁰

The equilibrium constants for PC (K_{PC}) and MM (K_{MM}) can be calculated from $\ln K_{\text{PC}} = \ln([\text{PC}_{\text{duplex}}]/[\text{PC}][\text{PR}]) = -(\Delta G_{\text{PC}}/RT)$ and $\ln K_{\text{MM}} = \ln([\text{MM}_{\text{duplex}}]/[\text{MM}][\text{PR}]) = -(\Delta G_{\text{MM}}/RT)$. Setting $[\text{MM}] = [\text{PC}]$ yields the energy criteria $-\Delta G_{\text{PC}} < 0$ and $-\Delta G_{\text{MM}} > 0$. This model is directly verified with the introduction of GNP-reporter as a way to measure inability of MM to open the hairpin probe.

The chips with nanoelectrodes were fabricated in two steps of lithography. On the first layer Ti/Au (thickness 50/150 Å) metal pads 500 nm apart were made using e-beam lithography and lift-off. In the second step, optical lithography was done to fabricate probing pads to contact the nanoelectrodes. Bare silicon chips were used to test the attachment and detection schemes prior to using nanoelectrode chips.

The chips were cleaned in oxygen plasma at 200 W in $\text{Ar} + \text{O}_2$ and Piranha solution, followed by surface attachment of probe DNA in a nitrogen glovebox with controlled ambi-

ence and temperature, as previously reported.¹³ The surface-attached probe molecules were heat cycled in TE buffer three times to ensure all molecules formed hairpin loop structures. The GNP-reporter conjugates were prepared using thiol-gold chemistry.¹⁴ The functionalized chips were immersed in TE buffer (pH 7.4) containing target DNA, either PC-target or MM-target, at a concentration of $2 \text{ fmol}/\mu\text{l}$ for 24 h at 40°C , followed by rinse with methanol and de-ionized water. Chips were then incubated in TE solution containing GNP-reporter. The GNP-reporter binds to the stem region of the probe toward the chip surface when it becomes available on binding of PC with probe (and is unavailable otherwise). In addition to the “PC” and “MM” chips, two control chips were used: (1) probe-functionalized chips not exposed to any target and (2) chips lacking probe and exposure to target DNA (i.e., silane SAM surface chemistry only). Control chips were incubated with GNP-reporter sequence as above. Neither control chip showed attachment of the GNP-reporter sequence.

The GNPs on the surface of control, MM, and PC exposed bare silicon chips were visualized by scanning electron microscopy (SEM) and manually counted using ImageJ software.¹⁵ The GNP count data were normalized as number of GNPs per square micron in Table II. The data clearly shows an order difference in the number of GNPs captured by the probe in case of PC-target than for MM-target, and a negligible number for control chips (Inset to Fig. 2).

Probing of control, MM, and PC nanoelectrode chips with the Agilent 4155C semiconductor parameter analyzer with a sweep of -1 to $+1$ V showed a significant difference between the PC and MM chips (Fig. 2). The current-voltage (I - V) measurements on MM chips showed a slight increase in conductivity (within the same order) in $\sim 3\%$ of the nano-

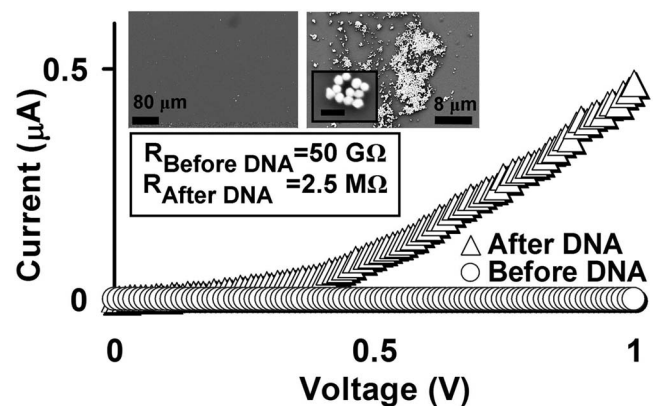


FIG. 2. Comparison of I - V data for a representative nanogap before hybridization of PC-target and probe (circles) and after exposure and hybridization of probe to PC-DNA and GNP-reporter (triangles). Insets: Left image shows chip with probe+MM-target+GNP-reporter. Right image shows chip with probe+PC-target+GNP-reporter. The inset to right micrograph shows the details of GNP-reporter payload on bare silicon chips (scale bar: 400 nm).

TABLE II. Count of average number of GNPs on silicon surfaces.

DNA Complexes	Mean number of particles/ μm^2	Standard deviation
Hairpin Probe+PC-target+GNP-reporter	11.62	5.60
Hairpin Probe+MM-target+GNP-reporter	0.86	0.76
Hairpin Probe+GNP-reporter (Control)	0.10	0.09
Silane SAM+GNP-reporter (Control)	0.01	0.00

electrode pairs. On the other hand, more than 70% of nano-electrode pairs showed a robust increase in conductivity on the PC-exposed chips. There were three orders of reduction in the resistance between the nanoelectrodes for PC-DNA (and amplified by GNP-reporter). The presence of GNPs provide charge-hopping sites to carriers, thus acting as a transduction block for the binding of PC with the probe. The tunneling current in a system of the nanogap electrodes with insulator (vacuum) between them can be approximately described by the Simmons formula as

$$J = \left(\frac{\alpha}{\delta_z^2} \right) \{ \bar{\varphi} \exp(-A \delta_z \sqrt{\bar{\varphi}}) - (\bar{\varphi} + eV) \exp[-A \delta_z \sqrt{\bar{\varphi} + eV}] \}$$

where $\alpha = e/(4\pi^2\beta^2\hbar)$, $A = 2\beta\sqrt{2m/\hbar^2}$, $\bar{\varphi}$ is the average barrier height relative to Fermi level of the negative electrode, δ_z is the barrier width, and eV represents the applied voltage across the nanoelectrodes.¹⁶ β is the dimensionless correction factor, e and m are the charge and mass of electron respectively, and \hbar is Dirac's constant. At small voltages when $\bar{\varphi} \gg eV$, the Simmons formula simplifies as $J = (\gamma\sqrt{\bar{\varphi}V}/\delta_z) \exp(-A\delta_z\sqrt{\bar{\varphi}})$, where $\gamma = (e\sqrt{2m})/(4\beta\pi^2\hbar^2)$. In the case of small voltages, the barrier height $\bar{\varphi}$ becomes independent of the applied voltage and the tunneling current becomes linearly dependent only on the applied voltage.¹⁷ The tunneling current characteristic can thus be modeled as two electrodes with high resistance between them. As the PC-target binds between these electrodes and GNP-reporter brings in GNPs, electrons find a lower barrier and thus start tunneling efficiently. Such framework shows the potential of electrical conductivity in microarrays.

The SEM imaging of the MM and PC nanoelectrode chips also confirmed the validity of the I - V measurements (Fig. 3). The images showed clusters of GNPs on PC-target chips between the nanoelectrodes, which provided the pathways for increased current through otherwise insulating electrodes. SEM micrographs also showed a negligible number of GNPs on the surface of MM-DNA chips. The few GNPs on the MM chips can be attributed to physical adsorption.

In summary, we present that the DNA-of-interest target molecules can be electrically detected using engineered hairpin probes. The detection of hybridization events can be amplified by using a GNP-reporter sequence complementary to stem region of the hairpin probe. The presence of GNP between electrodes enhances the conductivity between otherwise insulated nanoelectrodes. The GNP-reporter can be modeled as a circuit breaker demonstrating electrical quantification of the molecular interactions. The device has the

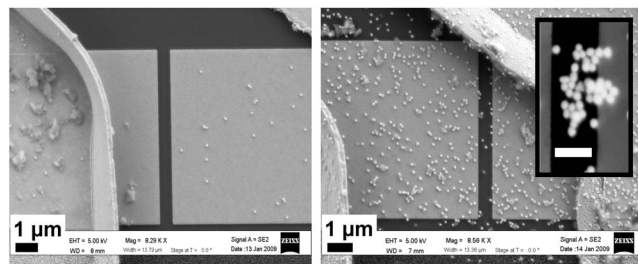


FIG. 3. SEM micrographs of nanoelectrode chips show side by side comparison of the amount of GNP in case of MM-target (left) and PC-target (right). There is a distinct difference in the GNP densities. Inset to right image shows closeup images of GNPs bridging the gap between the nanoelectrodes, causing the increase in conductivity for PC-target (scale bar: 400 nm).

potential to function as a traditional microarray but without the need to directly tag either the probe or target molecules.

This work was supported by funds from Research Enhancement Program at University of Texas at Arlington and National Science Foundation CAREER grant to S.M.I. (ECCS 0845669). The authors would like to thank Fatima Z. Amir for help with electron microscopy. Mohammad R. Noor and Swati Goyal contributed equally to this work.

- ¹K. L. Gorringer, S. Jacobs, E. R. Thompson, A. Sridhar, W. Qiu, D. Y. H. Choong, and I. G. Campbell, *Clin. Cancer Res.* **13**, 4731 (2007).
- ²P. A. Futreal, L. Coin, M. Marshall, T. Down, T. Hubbard, R. Wooster, N. Rahman, and M. R. Stratton, *Nat. Rev. Cancer* **4**, 177 (2004).
- ³M. Huncharek, J. Muscat, and J.-F. Geschwind, *Carcinogenesis* **20**, 1507 (1999).
- ⁴R. Etzioni, N. Urban, S. Ramsey, M. McIntosh, S. Schwartz, B. Reid, J. Radich, G. Anderson, and L. Hartwell, *Nat. Rev. Cancer* **3**, 243 (2003).
- ⁵E. E. Merkina and K. R. Fox, *Biophys. J.* **89**, 365 (2005).
- ⁶Y. S. Liu, P. P. Banada, S. Bhattacharya, A. K. Bhunia, and R. Bashir, *Appl. Phys. Lett.* **92**, 143902 (2008).
- ⁷J. Zhang, S. Song, L. Wang, D. Pan, and C. Fan, *Nat. Protoc.* **2**, 2888 (2007).
- ⁸S. R. Mikkelsen, *Electroanalysis* **8**, 15 (1996).
- ⁹T. Willner and M. Zayats, *Angew. Chem., Int. Ed.* **46**, 6408 (2007).
- ¹⁰F. Wei, B. Sun, W. Liao, J. Ouyang, and X. Sheng Zhao, *Biosens. Bioelectron.* **18**, 1149 (2003).
- ¹¹Y. Jin, X. Yao, Q. Liu, and J. Li, *Biosens. Bioelectron.* **22**, 1126 (2007).
- ¹²Gene Runner Software, version 3.01, Hastings Software, www.generunner.net.
- ¹³S. M. Iqbal, D. Akin, and R. Bashir, *Nat. Nanotechnol.* **2**, 243 (2007).
- ¹⁴J. J. Storhoff, R. Elghanian, R. C. Mucic, C. A. Mirkin, and R. L. Letsinger, *J. Am. Chem. Soc.* **120**, 1959 (1998).
- ¹⁵ImageJ Software, National Institutes of Health, USA, <http://rsb.info.nih.gov/ij/>.
- ¹⁶W. Wang, T. Lee, and M. A. Reed, *Phys. Rev. B* **68**, 035416 (2003).
- ¹⁷John G. Simmons, *J. Appl. Phys.* **34**, 1793 (1963).